Exploiting Chaotic Dynamics for A-D Converter Testing

Tommaso Addabbo, Ada Fort, S.Rocchi, Valerio Vignoli

Department of Information Engineering
University of Siena, 53100 Italy
(e-mail: addabbo@dii.unisi.it)

⋆ RESEARCH MANUSCRIPT ⋆

– PLEASE REFER TO THE PUBLISHED PAPER[1] –

Abstract

In this paper we discuss the possible use of chaotic signals for testing Analog-to-Digital Converters (ADCs), with particular reference to the well known Code Density Test (CDT, also called Histogram Test). In detail, we discuss the implementation of a chaos-based discrete-time noise generator circuit, providing the theoretical analysis of its statistical characterization. The implementation of the chaos-based device is discussed with reference to a generic hardware architecture, taking into account the nonidealities introduced by the the presence of noise and the variability of the circuit parameters. Based on this device, we propose a method for generating noisy samples that are distributed, over a target subinterval of the circuit output range, according to a probability density function (pdf) that can be made arbitrarily close to the ideal uniform pdf, while paying an acceptable reduction of the uniform-distributed samples generation rate. Theoretical results, also supported by two experiments, confirm the reliability of the proposed solution, showing that chaotic systems can represent an alternative with respect to traditional methods for the generation of signals to be used in the Code Density Test of ADCs.

1 Introduction

In this paper we discuss the possible use of chaotic signals for testing ADCs, with particular reference to the well known Code Density Test (CDT, also called Histogram Test) [1–3]. In detail, we discuss the implementation of a chaos-based discrete-time noise generator circuit, providing the theoretical analysis of its statistical properties. The implementation of the chaos-based device is discussed with reference to a generic hardware architecture, taking into account the nonidealities introduced by the the presence of noise and the variability of the circuit parameters. Based on this device, we propose a method for generating

[1]International Journal of Bifurcation and Chaos, 2010, vol. 20, n. 4, p. 1099-1118

noisy samples that are distributed, over a target subinterval of the circuit output range, according to a probability density function (pdf) that can be made arbitrarily close to the ideal uniform pdf, while paying an acceptable reduction of the uniform-distributed samples generation rate.

Paper organization: The original contribution of this work is reported in Sections 4-8, whereas the aim of Sections 2 and 3 is to make the paper self-contained, presenting the notation and some general definitions used through the paper. In detail, for the generation of noisy samples in Section 4 we propose to consider the Sawtooth chaotic map, deeply investigated in [4,5]. The main idea is to exploit the ergodic stochastic process generated by this dynamical system as a source of almost-uniform distributed samples for the CDT. In Section 5 we define a theoretical method for evaluating the distribution of the samples generated by a generic ergodic source. The study takes into account also the presence of noise in the analog circuit implementing the system, and the issue is treated in detail in Section 6. The method is then used in Section 7 for assessing the accuracy of the CDT when adopting the Sawtooth chaotic system as a test signal source. The validity of the theoretical results is supported by two experiments, reported in Section 8. Conclusions close the paper.

2 Notation

We denote with the interval $[V_{\min}, V_{\max}) \subset \mathbb{R}$ the *input domain* of the ADC, whereas we denote with $V_{FS} = V_{\max} - V_{\min}$ its *full scale range*. It is often convenient to express the transfer function of ADCs in terms of *code transition levels* $V_T(1), \ldots, V_T(N)$. The code transition levels define the *code bins*: the first bin, labeled with 0, is related to the subset of input values $x < V_T(1)$. The k-th code bin, for $k = 1, \ldots, N-1$, is the interval such that $V_T(k) \leq x < V_T(k+1)$, whereas the last code bin, labeled with N, identifies the subset $x \geq V_T(N)$. For $k = 1, \ldots, N-1$ the k-th code bin has width

$$W(k) = V_T(k+1) - V_T(k), \tag{1}$$

and for an ideal ADC we have $N = 2^n - 1$ and each code bin has width $Q = \frac{V_{\max} - V_{\min}}{2^n} = \frac{V_{FS}}{2^n}$.

2.1 Static Errors in non-ideal ADCs

Concerning non-ideal ADCs, in this paper we refer to the following definitions [1,3]:

- *Nominal average code bin width* $\overline{Q}$: in real n-bit ADCs the transition levels are not uniformly spaced in the input domain. Accordingly, the code bins have different widths, and the nominal average code bin width $\overline{Q}$ is defined as

$$\overline{Q} = \frac{V_T(N) - V_T(1)}{2^n - 2}. \tag{2}$$

  In this paper the *mid-riser* convention is adopted, i.e., $V_{\min} = V_T(1) - \overline{Q}$ and $V_{\max} = V_T(N) + \overline{Q}$.

- *Gain and Offset*: These quantities can be obtained by computing a linear regression based on the general relationship [3]

$$\Gamma \cdot V_T(k) + V_{OS} + r(k) = (k-1) \cdot \overline{Q} + V_T(1), \tag{3}$$

for $k = 1, \ldots, N$. In (3) Γ is the gain, V_{OS} is the offset and $r(k)$ is a residual error. The linear regression can be calculated according to several methods, e.g., in order to minimize the sums of the square of the residuals $\sum_k r^2(k)$. In such case Γ and V_{OS} can be determined solving a simple linear system [1].

- *Integral nonlinearity*: Once determined the static gain and offset by means of (3), the static integral nonlinearity (INL) (as a function of $k = 1, \ldots, N$) is given by the ratio

$$\mathrm{INL}(k) = \frac{r(k)}{\overline{Q}}. \tag{4}$$

The INL error for an ADC, denoted with $\mathrm{INL}_{\max}$, is assumed to be equal to the maximum of $|\mathrm{INL}(\cdot)|$.

- *Differential nonlinearity*: After correcting for static gain, the differential nonlinearity (DNL) is the difference between the width of a specified code bin and the average code bin width $\overline{Q}$, divided by $\overline{Q}$, i.e.,

$$\mathrm{DNL}(k) = \frac{\Gamma \cdot W(k) - \overline{Q}}{\overline{Q}}, \qquad k = 1, \ldots, N-1. \tag{5}$$

The differential nonlinearity error for an ADC, denoted with $\mathrm{DNL}_{\max}$, is identified with the maximum of $|\mathrm{DNL}(\cdot)|$, and the DNL error for an ideal ADC is zero.

According to the above definitions, both DNL and INL errors are defined as fractions of $\overline{Q}$, and an ideal ADC has $\Gamma = 1$, $V_{OS} = 0$, $\mathrm{INL}_{\max} = 0$ and $\mathrm{DNL}_{\max} = 0$. Moreover, when the ADC exhibits a negligible offset and gain error, an approximated expression for the INL and DNL errors can be obtained assuming $\Gamma \approx 1$ and $V_{OS} \approx 0$. In such case, from (5) it results that $W(k) \approx \overline{Q}(\mathrm{DNL}(k) + 1)$, and it is easy to prove that $r(k) \approx (k-1)\overline{Q} - \sum_{i=1}^{k-1} W(i)$, and

$$\mathrm{INL}(k) \approx k - 1 - \sum_{i=1}^{k-1} \frac{W(i)}{\overline{Q}} \approx -\sum_{i=1}^{k-1} \mathrm{DNL}(i). \tag{6}$$

3 The Code Density Test (CDT)

Assuming the ADCs under test monotonic and not affected by hysteresis[2], the CDT is briefly reviewed in the following: many samples of an ergodic stochastic sequence (e.g., a randomly sampled sinusoid[3]) are A-D converted, and an histogram of output code occurrences is then generated. Due to the ergodicity

[2] Indeed, these non-idealities can cause the Code Density Test producing erroneous results [1].

[3] In literature, the random sampling of sine or triangle waves has been widely investigated [1, 3].

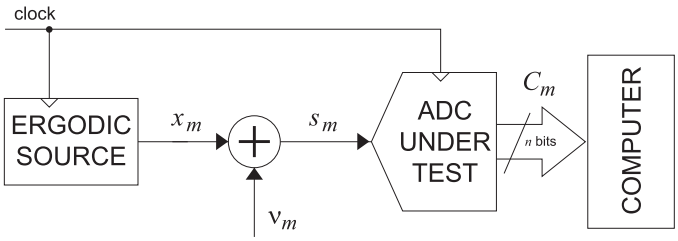


Figure 1: The general setup schematic model for the Code Density Test.

of the input sequence, in the limiting case of an infinite number of samples, the relative number of counts occurring for a given code k is equal to the probability for an input sample to belong to the k-th code bin. According to the general test setup model shown in Fig. 1, if the probability density function (pdf) ρ of the ADC input samples $\{s_m\}$ is known, the following limit is satisfied

$$\lim_{S_\# \to \infty} \frac{h_S(k)}{S_\#} = \int_{V_T(k)}^{V_T(k+1)} \rho(x)dx, \tag{7}$$

where $S_\#$ is the number of input samples, and $h_S(k)$ is the number of samples falling in the k-th code bin. The validity of eq. (7) can be extended to the whole set of code bins assuming $V_T(0) = -\infty$ and $V_T(N+1) = +\infty$.

The ADC input samples $\{s_m\}$ are collected from the output of an ergodic source with proper statistical features. In the ideal noiseless case, referring to Fig. 1, we have that at each step m the pdf ρ of the random variable s_m is equal to the pdf ϕ of x_m. Actually, in analog circuits the samples $\{x_m\}$ are affected by noisy perturbations, and the pdf ρ is given by the convolution[4]

$$\rho(x) = (\phi \otimes f_\nu)(x) = \int_{-\infty}^{+\infty} \phi(x-\theta) f_\nu(\theta) d\theta, \tag{8}$$

where f_ν is the stationary pdf of the noise process.

In general, from (7) we obtain the expression

$$\lim_{S_\# \to \infty} \frac{1}{S_\#} \sum_{i=0}^{k} h_S(k) = \int_{-\infty}^{V_T(k+1)} \rho(\theta) d\theta, \tag{9}$$

which relates the transition levels and the code occurrences. Depending on the pdf ρ, from (9) a direct reversed expression for $V_T(k+1)$ can be computed, i.e., a proper function $\Psi : [0,1) \to [V_{\min}, V_{\max})$ can be determined such that

$$V_T(k+1) = \lim_{S_\# \to \infty} \Psi \left(\frac{1}{S_\#} \sum_{i=0}^{k} h_S(k) \right). \tag{10}$$

On the basis of (10) an estimator for the transition levels can be defined for determining the static AD characteristic function. E.g., when the input samples

[4]The noisy perturbation signal is supposed to be an ergodic process statistically independent from the input.

are uniformly distributed over the interval $[L_{\min}, L_{\max})$, with $L_{\min} < V_T(1)$ and $L_{\max} > V_T(N-1)$ expression (10) has the simple form

$$V_T(k) = L_{\min} + \lim_{S_\# \to \infty} \frac{L_{\max} - L_{\min}}{S_\#} \sum_{i=0}^{k-1} h_S(i). \tag{11}$$

Concerning the estimation of the code transition levels, we classify two types of estimation errors that must be taken into account:

E1 errors: these are the statistical errors introduced when truncating the infinite sequence used for computing the argument of function Ψ (indeed, the number of samples being converted in the CDT is necessarily finite);

E2 errors: these are the statistical errors due to the uncertainties about the knowledge of the pdf ρ.

REMARK: In this paper we focus on the E2 errors (since the E1 errors can always be reduced to arbitrary levels *by increasing the number of samples used in the CDT*).

4 The Chaotic Source

Referring to the scheme shown in Fig. 1, in this paper we assume the samples $\{x_m\}$ generated by a chaotic source implemented by the block diagram in Fig. 2. In this diagram, five different analog blocks are used to determine the sample z'_{m+1} as a function of z'_m: a comparator, an adjustable gain block, one adder, a ± 1 constants generator, and a delay block τ. The logic variable Y_m obtained at the output of the comparator assumes the value '1' if $z'_m \geq P$, and the value '0' otherwise. Furthermore, one amplifier and one adder are used for obtaining the final output signal x_m. In this circuit, the chaotic dynamics is ruled by the transformation

$$z'_{m+1} = \begin{cases} Bz'_m + 1, & \text{if } z'_m < P, \\ Bz'_m - 1, & \text{if } z'_m \geq P, \end{cases} \tag{12}$$

with $B \in \mathbb{R}^+$ and $P \in \mathbb{R}$. The sequence $\{x_m\}$ of output samples is obtained as

$$x_m = G(z'_m + \Delta), \tag{13}$$

with $G \in \mathbb{R}^+$ and $\Delta \in \mathbb{R}$.

As discussed in the following subsections, by properly setting the parameters P, B, G and Δ, the above system can generate samples uniformly distributed over any limited interval of the form $[L_{\min}, L_{\max})$.

4.1 The Sawtooth chaotic dynamics

We briefly recall the main properties of the chaotic dynamical system (12).For values of the system parameters satisfying

$$\begin{cases} 0 \leq |P| < \frac{2-B}{B^2-B}, \\ \sqrt{2} < B \leq 2, \end{cases} \tag{14}$$

the dynamics is chaotic over the attractor $[BP - 1, BP + 1)$, i.e., any initial condition z'_0 chosen within the interval delimited by the two fixed points

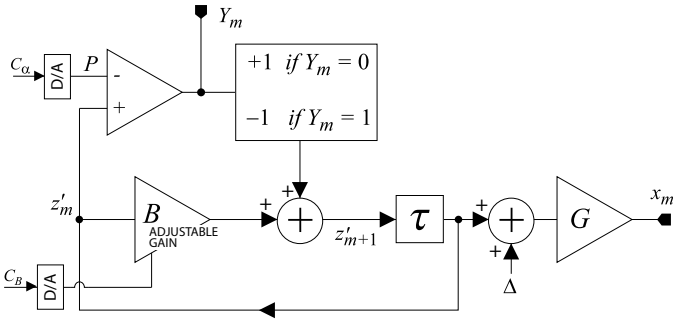


Figure 2: Block scheme of the mixed analog-digital circuit based on the Sawtooth map generating the ergodic output samples for the CDT.

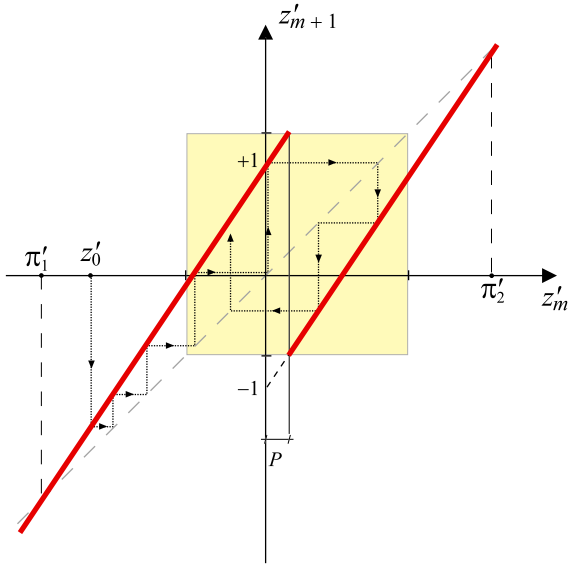


Figure 3: The map (12) for $B = 1.51$ and $P = 0.23$. The first seven iterations of the sequence $\{z'_m\}$ triggered by the initial condition z'_0 is also reported. The gray area bounds the chaotic attractor $[BP - 1, BP + 1)$.

$(\pi_1', \pi_2') = (\frac{-1}{B-1}, \frac{1}{B-1})$ triggers a chaotic trajectory $\{z_m'\}$ eventually trapped in the chaotic attractor $[BP-1, BP+1)$. The statistical characterization of the dynamics depends on the system parameters B and P.

In [4, 5] it was proved that the dynamical system (12) can be conveniently studied taking into account the chaotic map

$$z_{m+1} = T(z_m) = \begin{cases} B(z_m - \alpha) + 1 & \text{if } z_m < \alpha, \\ B(z_m - \alpha) - 1 & \text{if } z_m \geq \alpha, \end{cases} \tag{15}$$

where $\alpha = P(1-B)$. System (15) and (12) are topologically conjugated by a linear homeomorphism and the dynamics of (15) is obtained shifting the dynamics of (12) by a quantity $-BP$, i.e.,

$$z = z' - BP. \tag{16}$$

The main advantage of the equivalent form (15) with respect to (12) consists in a dynamics that is always referred to the chaotic attractor $\Lambda = [-1, 1)$, regardless of the variation of the system parameters B and P.

The dynamical behavior of system (15) is completely determined by its parameters B and α, and in the following we refer to (15) as the *Sawtooth dynamical system*. The relationship between α, B and P can be used for translating the parameter space (14) into an equivalent parameter space for the system (15). In detail, in [4] it was proved that for

$$\begin{cases} 0 \leq |\alpha| < 0.17, \\ \sqrt{2} < B \leq \frac{2}{1+|\alpha|}, \end{cases} \tag{17}$$

the Sawtooth map is an exact transformation over the attractor $\Lambda = [-1, +1)$, i.e., any initial condition z_0 chosen within the interval delimited by the two fixed points $(\pi_1, \pi_2) = (\frac{B\alpha-1}{B-1}, \frac{B\alpha+1}{B-1})$ triggers a chaotic trajectory $\{z_m\}$ eventually trapped into the interval $\Lambda = [-1, +1)$ that exhibits the most complex behavior classified in Ergodic Theory [4, 6]. As depicted in Fig. 4, for $B > \frac{2}{1+|\alpha|}$ almost all initial conditions trigger sequences eventually attracted toward plus or minus infinity[5], whereas for $B \leq \sqrt{2}$ the map loses its exact property [4, 5, 8]. In this paper, we assume the system parameters B and α belonging to the parameter space defined in (17).

It is interesting noting that if $P = \alpha = 0$ systems (15) and (12) are identical; moreover, according to the parameter spaces (14) and (17), in both cases the parameter B can be set equal to 2 only if $P = \alpha = 0$.

4.2 Theoretical setup

We adopt the following notation and terminology. Let $I \subset \mathbb{R}$ be an interval. We denote with $\mathcal{B}_I$ the usual Borel σ-algebra of subsets of I, and with $\lambda : \mathcal{B}_I \to \mathbb{R}^+$ the Lebesgue measure. We say that a property holds almost everywhere (a.e.) on I if the subset $F \subset I$ on which the property fails has zero measure, i.e., $\exists H \in \mathcal{B}_I$ such that $F \subseteq H$ and $\lambda(H) = 0$. With reference to the Lebesgue integration theory, the notation $L^p(I)$ denotes the set of functions $f : I \to \mathbb{R}$

[5] In such case we say that the dynamics diverges. As discussed in [7], in real electronic circuits this condition leads the dynamics to stabilize on parasitic saturation equilibrium points.

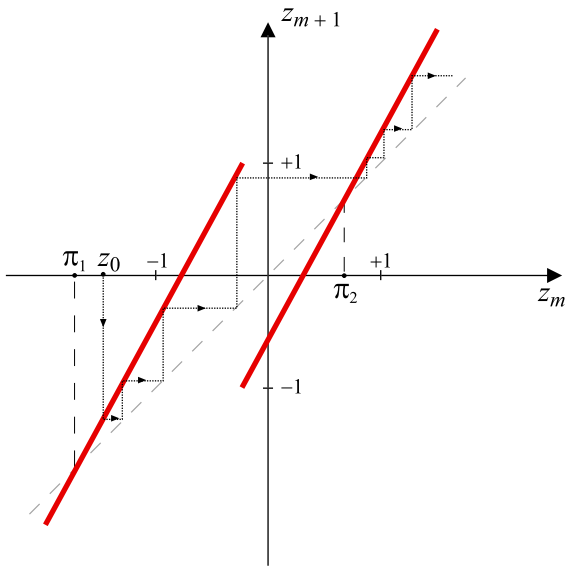


Figure 4: A diverging trajectory for the Sawtooth map (15) with $B > \frac{2}{1+|\alpha|}$.

such that $\int_I |f(x)|^p dx < \infty$, with $0 < p \in \mathbb{N}$, whereas $L^\infty(I)$ is the set of a.e. bounded measurable functions. We recall that $L^p(I)$ and $L^\infty(I)$ can be made Banach spaces with reference to the norms $\|f\|_p = (\int_I |f(x)|^p dx)^{\frac{1}{p}}$ and $\|f\|_\infty = \inf\{M \in \mathbb{R}^+ \text{ such that } \{x \in I : |f(x)| > M\} \text{ has zero measure}\}$, respectively.

We define $\mathcal{P}_I$ as the set of all finite partitions of intervals[6] of I, and if $Q \in \mathcal{P}_I$, we denote the endpoints of Q with $\mathcal{E}_Q = \{p_0, \ldots, p_q\}$, with $p_i < p_j$ if $i < j$. If there exists a positive number M such that $\forall Q \in \mathcal{P}_I$

$$V_I(f, Q) = \sum_{k=1}^{\#Q} |f(p_k) - f(p_{k-1})| \leq M, \tag{18}$$

then f is said to be of *bounded variation* on I and the quantity $V_I(f) = \sup_{\mathcal{P}_I}\{V_I(f, Q)\}$ is the *total variation* of f on I.

We can now define the following subset of $L^1(I)$

$$BV(I) = \{f \in L^1(I) : \\ \exists g \in L^1(I) \text{ such that } V_I(g) < \infty \text{ and } g = f \text{ a.e.}\}. \tag{19}$$

Note that $BV(I)$ also contains functions with infinite variation that are a.e. equal to a bounded variation function. In such case we define the *infimum total variation* of $f \in BV(I)$ as $\tilde{V}_I(f) = \inf\{V_I(g) : g \in BV(I), g = f \text{ a.e.}\}$. The set $BV(I)$ is a vector space of functions, which can be made a Banach space with the norm $\|f\|_{BV} = \|f\|_1 + \tilde{V}_I(f)$, and it can be proved that that $BV(I)$ is dense in $L^1(I)$ [8]. Finally, we define the subset of pdfs as $D_1(I) = \{f \in L^1(I) :$

[6] If $P \in \mathcal{P}_I$ then $P = \{I_i, i = 1, \ldots, p, \text{with } p > 0\}$, with $I_i \cap I_j = \oslash$ for $i \neq j$, and $\cup_{i=1}^p I_i = I$.

$\|f\|_1 = 1\}$ and we introduce the subset $D_{BV}(I) = BV(I) \cap D_1(I)$. Finally, we recall that if $f : I \to \mathbb{R}$ then $\operatorname{ess\,sup} f = \inf\{a \in \mathbb{R} : \lambda(x : f(x) > a) = 0\}$ and, conversely, $\operatorname{ess\,inf} f = \sup\{a \in \mathbb{R} : \lambda(x : f(x) < a) = 0\}$.

REMARK: in the following we deal with pdfs of bounded variation $\phi \in D_{BV}(I)$. We stress that this set of functions is dense in the set of pdf $D_1(I)$, and that it contains all the pdfs of practical interest. For example, all the bounded pdfs $\phi : I \to \mathbb{R}^+$ continuous on I, or with a finite number of discontinuities, belong to $D_{BV}(I)$.

4.3 Ergodic behavior of the Sawtooth dynamical system

In this subsection we briefly discuss the chief ergodic properties of the Sawtooth dynamical system, whereas a deeper theoretical study can be found in [4] and in the references cited therein.

It is worth underlining that for a chaotic map the sensitivity of the dynamics to the initial condition physically manifests itself, as the time passes, as an exponential growth of the uncertainty about the prediction of the dynamical evolution [9]. Accordingly, the repeated iteration of the deterministic transformation T defined in (15) can be used for defining a stochastic process $\{z_0, z_1, \ldots\}$, where $z_{m+1} = T(z_m)$, once assuming the initial condition z_0 as a *random variable*. Accordingly, the uncertain knowledge of the initial condition z_0 is described by a pdf ϕ_0 defined over the phase space Λ and, in general, we can describe the uncertain knowledge of the dynamical system state z_m specifying the absolutely continuous probability measure $\mu : \mathcal{B}_\Lambda \to [0, 1]$ defined as

$$\mu(J) = \int_J \phi_m(z)dz, \qquad J \in \mathcal{B}_\Lambda, \tag{20}$$

where the pdf $\phi_m : \Lambda \to \mathbb{R}^+$ belongs to $D_{BV}(\Lambda)$.

Among the theoretical tools at disposal to evaluate the evolution of pdfs under the repeated iterations of a discrete time chaotic system, the Frobenius Perron Operator is a fundamental one [6, 8]. In detail, for the system (15) we define this operator as $\Theta_T : D_{BV}(\Lambda) \to D_{BV}(\Lambda)$, where [6]

$$\begin{aligned} &\Theta_T\phi(x) = \\ &= \begin{cases} \frac{1}{B}\phi\left(\frac{x+1}{B} + \alpha\right), & \text{if } x \in J_1, \\ \frac{1}{B}\left[\phi\left(\frac{x-1}{B} + \alpha\right) + \phi\left(\frac{x+1}{B} + \alpha\right)\right], & \text{if } x \in J_2, \\ \frac{1}{B}\phi\left(\frac{x-1}{B} + \alpha\right), & \text{if } x \in J_3, \end{cases} \end{aligned} \tag{21}$$

with

$$\begin{aligned} J_1 &= [-1, -B(1+\alpha)+1), \\ J_2 &= [-B(1+\alpha)+1, B(1-\alpha)-1), \\ J_3 &= [B(1-\alpha)-1, 1). \end{aligned} \tag{22}$$

Accordingly, if $\phi_0 \in D_{BV}(\Lambda)$ is the pdf for z_0, the function $\phi_1 = \Theta_T\phi_0$ describes the distribution of the random state variable $z_1 = T(z_0)$. If Θ_{T^m} is the Frobenius-Perron operator corresponding to the iterated map $T^m = T \circ \overset{m}{\cdots} \circ T$, then $\Theta_{T^m} = \Theta_T \circ \overset{m}{\cdots} \circ \Theta_T$. Therefore, the pdf ϕ_m associated with the random state variable $z_m = T^m(z_0)$ can be obtained as $\phi_m = \Theta_T^m\phi_0$.

A pdf $\phi^* \in D_{BV}(\Lambda)$ is said *invariant* with respect to T iff $\Theta_T \phi^* = \phi^*$ a.e., and in such case (20) defines an *invariant probability measure*. Referring to the parameter space (17), in [4] it was proved that the Sawtooth map admits one unique invariant pdf $\phi^* \in D_{BV}(\Lambda)$, and that if $\phi_0 = \phi^*$ then the stochastic process $\{z_m\}$ is ergodic.

For exact systems like (15) it is not necessary to have $\phi_0 = \phi^*$, since they are *statistically stable* [6, 8], i.e., $\forall \phi_0 \in D_{BV}(\Lambda)$ we have that

$$\lim_{m \to \infty} \|\Theta_T^m \phi_0 - \phi^*\|_1 = 0. \tag{23}$$

The statistical stability derives from the inequality

$$\|\Theta_T^m \phi_0 - \phi^*\|_p \leq C r^m, \qquad 1 \leq p \leq \infty, \tag{24}$$

where C and r are positive constants that depend on ϕ_0 and T, with $0 < r < 1$ [8].

In other words, regardless of $\phi_0 \in D_{BV}(\Lambda)$ (i.e., regardless of the uncertainty level about the initial condition z_0), the statistical stability (23) assures that the stochastic dynamics ruled by the Sawtooth map (15) approaches an ergodic process with a convergence rate not slower than exponential. In [4] it was shown that the stochastic process ruled by the Sawtooth map can be assumed stabilized on its invariant stationary pdf after a limited number of iterations, e.g., a few dozen steps (Fig. 5).

REMARK: according to the above discussion, in the following we assume the Sawtooth chaotic dynamical system stabilized on its invariant ergodic pdf ϕ^*. Due to the shift relationship that exists between the sequences $\{z_m\}$ and $\{z'_m\}$, in the following we denote the invariant pdf for the sequence $\{z'_m\}$ as $\phi_z^*(x') = \phi^*(x - BP)$.

5 The Sawtooth dynamical systems as a source of samples for the CDT

It is well known that the unique invariant pdf for the Sawtooth map with $B = 2$ and $\alpha = 0$ is uniform over $\Lambda = [-1, 1)$ [7]. Accordingly, by properly setting the parameters G and Δ in (13), the system implemented by the block-diagram in Fig. 2 can be used for generating samples uniformly distributed over any limited interval of the form $[L_{\min}, L_{\max})$. On these bases, in this paper we propose to use the Sawtooth map as a random source of samples for the CDT, as discussed in the following.

5.1 The shape of the invariant pdf

In analog electronic circuits a small deviation of the parameter values from their nominal design values is unavoidable in practice, and hence it is not possible to set B exactly equal to 2 while assuring, according to (17), α exactly equal to 0, avoiding the divergence of the dynamics. To avoid divergence, system (15) can be therefore used only for $B < \frac{2}{1+|\alpha|} < 2$, and the accurate determination of the invariant pdf ϕ^* for B values lower than 2 is mandatory for using the chaotic samples $\{z_m\}$ in the CDT of ADCs.

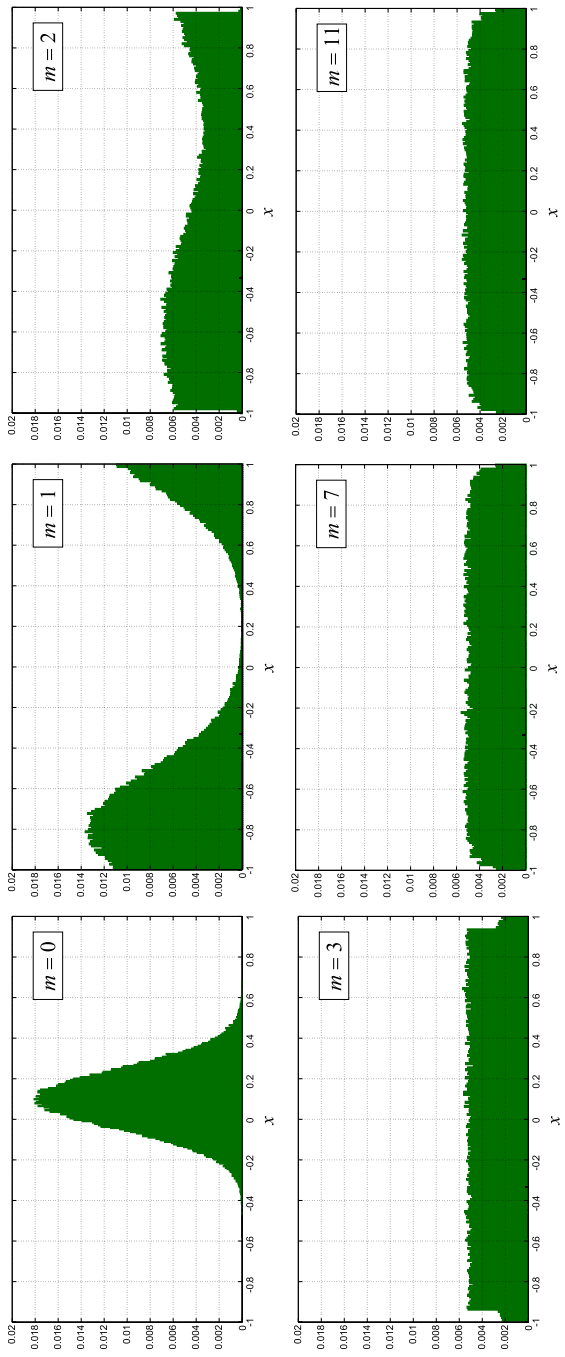


Figure 5: Evolution of the state pdf ϕ_m under the iterations of the Sawtooth map (15) with $B = 1.98$ and $\alpha = 0.002$, once assuming ϕ_0 as a gaussian pdf.

For $B < 2$, only in few cases the invariant pdf ϕ^* can be calculated analytically, whereas it can be always accurately estimated with numerical computations. In [4,10] an efficient method to numerically estimate the invariant measure for piecewise affine chaotic maps like (15) is proposed. With this method the invariant pdf for the Sawtooth map can be estimated for any given parameter set B, α with low-complex numerical computations, being the accuracy of the estimation theoretically guaranteed [4].

This method was used by the authors to calculate the invariant pdfs for several B and α values, as reported in the first row of Fig. 6. As it can be observed in this figure, as far as the parameter B gets close to 2, the ergodic pdf ϕ^* for the Sawtooth map better approximates an uniform pdf. This result has a theoretical explanation in the robustness property of the Sawtooth map invariant measure with respect to parameter perturbations [4], as stated in the following

Theorem 1 (Derived from [4]) *Let $\{B_n, \alpha_n\}$ be a sequence of values satisfying (17) for all $n \in \mathbb{N}$, and such that $\lim_{n\to\infty} B_n = 2$. Let ϕ_n^* be the unique invariant density of the Sawtooth map (15) with parameters B_n, α_n. Then the sequence $\{\phi_n^*\}$ strongly converges in $L_1(\Lambda)$ to the uniform pdf $f(x) = 0.5$, i.e.,*

$$\lim_{n\to\infty} \|\phi_n^* - 0.5\|_1 = 0. \tag{25}$$

It is worth remarking that (25) implies the convergence of probability measures, i.e., $\forall A \in \mathcal{B}_\Lambda$

$$\lim_{n\to\infty} \mu_n^*(A) = \lim_{n\to\infty} \int_A \phi_n^*(x)dx = 0.5 \cdot \lambda(A). \tag{26}$$

Since for B sufficiently close to 2 we deal with *'almost uniform'* pdfs, we are interested in introducing an easy and reliable method for evaluating and comparing different pdfs, in order to establish, for example, which one better approximates the uniform pdf. Accordingly, for a given arbitrary pdf $\phi \in D_{BV}(\Lambda)$ for $0 < x \leq 1$ we define the following quantities

$$\sup_\phi(x) = \operatorname{ess\,sup} \phi|_{[-x,x)}\,, \tag{27}$$

$$\inf_\phi(x) = \operatorname{ess\,inf} \phi|_{[-x,x)}\,, \tag{28}$$

where $\phi|_{[-x,x)}$ is the restriction of ϕ to the interval $[-x, x)$. Finally, the function

$$\overline{\phi}(x) = \frac{1}{2x} \int_{-x}^{x} \phi(z)dz \tag{29}$$

is the mean value of ϕ restricted to the interval $[-x, x)$. On the basis of the above equations, we have the following

Definition 1 *For the pdf ϕ the* uniformity error $E(\phi) : (0, 1] \to \mathbb{R}^+$ *is defined as*

$$E(\phi)(x) = \frac{\sup_\phi(x) - \inf_\phi(x)}{\overline{\phi}(x)}. \tag{30}$$

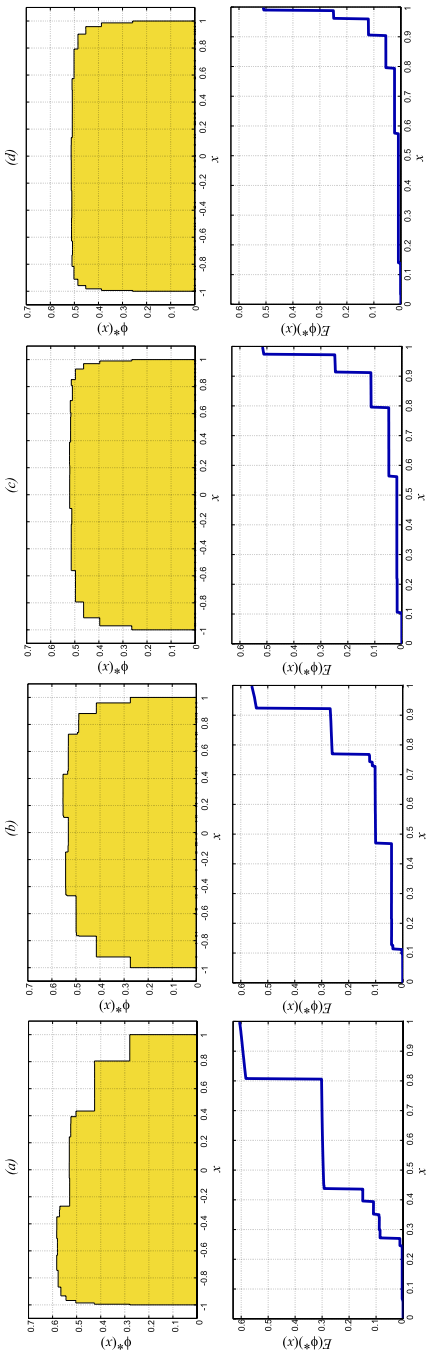


Figure 6: In the first row, the accurate estimation of the unique invariant pdf ϕ^* for system (15), with (a) $B = 1.9$, $\alpha = 0.05$, (b) $B = 1.94, \alpha = -0.01$, (c) $B = 1.98, \alpha = -0.005$ and (d) $B = 1.99, \alpha = 0.002$. In the second row, for each case, the plot of the respective quantity $E(\phi^*)(x)$ defined in (30).

As an example, the plots of the error function $E(\phi)$ computed for some ergodic pdfs ϕ^* obtained for different parameter values of the Sawtooth map are shown in the second row of Fig. 6. It is interesting noting that in general

$$\lim_{x\to 0^+} E(\phi)(x) = 0, \tag{31}$$

$$\lim_{x\to x_0^-} E(\phi)(x) = E(\phi)(x_0), \tag{32}$$

and that if ϕ is a perfect uniform pdf then $E(\phi)(x) = 0$ for all $x \in (0, 1]$.

The introduced error function $E(\phi)$ can be used for determining a subinterval of Λ, containing the origin $x = 0$, in which the restriction of the pdf ϕ can be assumed *'almost uniform'* up to a certain error $\varepsilon > 0$. In detail, we emphatize the correct interpretation of the function $E(\phi)$ introducing the

Definition 2 *Let $u \in (0, 1]$. Let $\phi_1, \phi_2 \in D_{BV}(\Lambda)$ and let $E(\phi_1), E(\phi_2)$ be their respective error functions (30). We say that on the interval $(-u, u)$ the pdf ϕ_2 is* better uniformly shaped *than the pdf ϕ_1 if and only if $E(\phi_2)(u) < E(\phi_1)(u)$.*

According to (31) the set $\{x \in (0, 1] : E(\phi)(x) \le \varepsilon\}$ is non-empty for any $\varepsilon > 0$. If we define

$$U_\varepsilon = \sup\{x \in (0, 1] : E(\phi)(x) \le \varepsilon\}, \tag{33}$$

it is easy to prove that due to (32) $E(\phi)(U_\varepsilon) \le \varepsilon$.

We have the following

Theorem 2 *Let $I \in \mathcal{B}_\Lambda$, with $I \subseteq (-U_\varepsilon, U_\varepsilon)$. Then*

$$\frac{\left|\mu(I) - \lambda(I)\overline{\phi}(U_\varepsilon)\right|}{\lambda(I)\overline{\phi}(U_\varepsilon)} \le \varepsilon. \tag{34}$$

Proof. From the definition (30) it results that

$$E(\phi)(U_\varepsilon) = \frac{\sup_\phi(U_\varepsilon) - \inf_\phi(U_\varepsilon)}{\overline{\phi}(U_\varepsilon)} \le \varepsilon. \tag{35}$$

The probability measure of I must satisfy the equation

$$\inf_\phi(U_\varepsilon)\lambda(I) \le \mu(I) \le \sup_\phi(U_\varepsilon)\lambda(I). \tag{36}$$

On the other hand, since $\overline{\phi}(U_\varepsilon)$ defined by eq. (29) is the mean value of ϕ restricted to $(-U_\varepsilon, U_\varepsilon)$, we have $\inf_\phi(U_\varepsilon) \le \overline{\phi}(U_\varepsilon) \le \sup_\phi(U_\varepsilon)$. Accordingly it results

$$\begin{aligned} \inf_\phi(U_\varepsilon)\lambda(I) - \sup_\phi(U_\varepsilon)\lambda(I) \le \\ \le \mu(I) - \overline{\phi}(U_\varepsilon)\lambda(I) \le \\ \le \sup_\phi(U_\varepsilon)\lambda(I) - \inf_\phi(U_\varepsilon)\lambda(I) \end{aligned} \tag{37}$$

and therefore, using (35),

$$\begin{aligned} 0 \le \left|\mu(I) - \overline{\phi}(U_\varepsilon)\lambda(I)\right| \le \\ (\sup_\phi(U_\varepsilon) - \inf_\phi(U_\varepsilon))\lambda(I) \le \varepsilon\overline{\phi}(U_\varepsilon)\lambda(I), \end{aligned} \tag{38}$$

concluding the proof. □

In the above inequalities the quantity $\overline{\phi}(U_\varepsilon)\lambda(I)$ represents the average probability measure of any subset with Lebesgue measure $\lambda(I)$, i.e., it is the measure of I assuming the restriction of the pdf ϕ to the domain $(-U_\varepsilon, U_\varepsilon)$ *constant and equal to its mean value* computed on $(-U_\varepsilon, U_\varepsilon)$. Accordingly, the quantity in the left side of inequality (34) represents, for the probability measure of I, the *fractional deviation* with respect to the *average probability measure* of any subset with Lebesgue measure $\lambda(I)$.

As far as the ergodic source based on the Sawtooth map is concerned, depending on ε the value U_ε can be numerically computed, once known the stationary pdf ϕ^*. It is interesting noting from Fig. 6 that, for any fixed ε, $U_\varepsilon \to 1$ as far as $B \to 2$. From a theoretical point of view, this is a consequence of the fact that ϕ^* tends to the uniform pdf as far as $B \to 2$ (Theor. 1).

Summarizing, the uniformity error function defined in (30) represents a tool for comparing two different pdfs ϕ_1 and ϕ_2 in terms of 'ideality': if for a certain u such that $0 < u \leq 1$ it results that $E(\phi_2)(u) < E(\phi_1)(u)$ then the pdf ϕ_2 is closer to the uniform pdf than ϕ_1 on $(-u, u)$, and for the probability measure of any measurable subset $I \subseteq (-u, u)$, the fractional error defined in (34), and associated to ϕ_2, is bounded by $E(\phi_2)(u)$. Indeed, (37) can be in general rewritten as

$$\begin{aligned} &\inf_\phi(u)\lambda(I) - \sup_\phi(u)\lambda(I) \leq \\ &\leq \mu(I) - \overline{\phi}(u)\lambda(I) \leq \sup_\phi(u)\lambda(I) - \inf_\phi(u)\lambda(I) \end{aligned} \tag{39}$$

which implies, using (30),

$$\begin{aligned} &0 \leq \left|\mu(I) - \overline{\phi}(u)\lambda(I)\right| \leq \\ &(\sup_\phi(u) - \inf_\phi(u))\lambda(I) = E(\phi)(u)\overline{\phi}(u)\lambda(I). \end{aligned} \tag{40}$$

5.2 Control of the Sawtooth map parameters

As it can be seen in Fig. 6, the shape of the invariant pdf for the Sawtooth map exhibits a high sensitivity to parameter changes, and a method for controlling B and α has to be taken into account. In [5] a feedback strategy to control and correct the Sawtooth map parameters has been proposed, with the aim of setting $|\alpha|$ below a small worst case $|\alpha|_{wc}$ while bringing the parameter B as much as possible close to 2, above the worst case value $B_{wc} = \frac{2}{1+|\alpha|_{wc}} < 2$. As discussed in [5], the correction is obtained by changing the parameters P and B in the block-diagram of Fig. 2. The controlling method, adapted for the CDT purpose, is briefly summarized in the Appendix.

6 Effects of Noise

In what follows we analyze the effects of noise by considering two distinct noise contributions, that are treated separately: the additive noise $\{\xi_m\}$ affecting the dynamics of the chaotic source (we call this *internal noise*) and the additive noise $\{\nu_m\}$ added at the output of the chaotic source (the *external noise*). This latter additive noise source is explicitly represented in Fig. 1.

6.1 Effects of the internal noise

Referring to the approach of Lasota in [6] the presence of internal noise can be modeled as it follows. At each time step the chaotic sample z_{m+1} deviates from its ideal value due to a statistically independent noise ξ_m added to the sample z_m, i.e.,

$$z_{m+1} = T(z_m + \xi_m). \tag{41}$$

It is worth noting that the presence of noise can cause the trajectories to diverge, e.g., bringing the perturbed state $z_m+\xi_m$ outside the basin of attraction of the chaotic attractor: in such case the resulting divergence event shown in Fig. 4 can occur also for $B < \frac{2}{1+|\alpha|}$. Accordingly, depending on the system parameter values and on the statistical distribution of the additive noisy samples $\{\xi_m\}$, we define the *confinement probability* at the time step m as the probability for the perturbed samples $\{z_i, i = 0, \ldots, m\}$ to be confined within the basin of attraction of the chaotic system, once assuming the sample z_0 distributed according to a pdf ϕ_0.[7] The resulting process is a complex discrete-time random walk on the real domain, which may not admit a stable stationary solution [6]. In general, assuming the noisy samples $\{\xi_m\}$ as i.i.d. random variables statistically independent from the $\{z_m\}$ samples, it results that

$$\phi_{m+1} = \tilde{\Theta}_T(\phi_m \otimes f_\xi) \tag{42}$$

where f_ξ is the pdf of bounded variation associated to the noisy samples, whereas the operator $\tilde{\Theta}_T : D_{BV}(\mathbb{R}) \to D_{BV}(\mathbb{R})$ is the extension of the Frobenius Perron operator Θ_T defined in (21) to the whole set of densities of bounded variations in $L^1(\mathbb{R})$. It is worth noting that z_m only depends on the noisy samples $\xi_{m-1}, \xi_{m-2}, \ldots$ and if $\phi = \tilde{\Theta}_T(\phi \otimes f_\xi)$ then the pdf ϕ is stationary and invariant for the stochastic dynamical system (41). The characterization of the evolution of densities (42) for systems like (41) is still an open theoretical problem, and depending on the considered case even the existence of an invariant density can be an undetermined issue [6, 11].

The consequence of the stochastic perturbations on the dynamics can be studied resorting to computer simulations, and in this subsection we discuss the effects of noise when using the chaotic Sawtooth map as an almost-uniformly distributed ergodic source for the CDT.

Assuming the process $\{\xi_m\}$ a white noise distributed according to a Gaussian distribution with zero mean and standard deviation σ_i, we denote with $3\sigma_{\max} = \frac{2+B(|\alpha|-1)}{B-1}$ the margin of safety[8] such that if z_m is in the attractor $\Lambda = [-1, 1)$ the probability for the perturbed state $z_m + \xi_m$ to escape from the basin of attractor when $\sigma_i = \sigma_{\max}$ is smaller than 0.2%. Different cases were simulated by varying σ_i and the system parameters B, α. The numerical analysis showed that if $\sigma_i < 0.6\sigma_{\max}$ the stochastic system behaves according to a process with high confinement probability (see, e.g. Fig. 7). As it can be seen in Fig. 7, for $\sigma_i \leq 0.6\sigma_{\max}$ the probability for a divergence event is practically negligible up to 10^6 map iterations.

[7] We recall that for the Sawtooth map (15) the basin of attraction of the attractor $\Lambda = [-1, 1)$ is the interval delimited by the two fixed points $(\pi_1, \pi_2) = (\frac{B\alpha-1}{B-1}, \frac{B\alpha+1}{B-1})$

[8] The quantity $3\sigma_{\max}$ is computed as the minimum distance between the border of the chaotic attractor $\Lambda = [-1, 1)$ and the fixed points π_1 and π_2. The quantity $3\sigma_{\max}$ approaches zero if $(B, \alpha) \to (2, 0)$, whereas it tends to increase as far as B drops below 2.

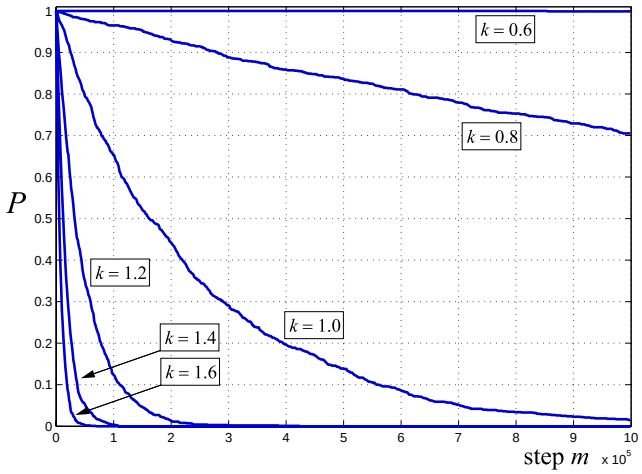


Figure 7: The confinement probability estimated for the Sawtooth map with $B = 1.98$ and $\alpha = 0.001$, considering different values of the white noise standard deviation $\sigma_i = k\sigma_{\max}$. Each case was estimated on the basis of a 1000 Monte Carlo simulation assuming z_0 uniformly distributed over $\Lambda = [-1, 1)$.

If the margin of safety is large enough to avoid divergence events the evolution of densities (42) stabilizes on an invariant pdf ϕ^* (Fig. 8) according to a converging rate comparable with the one of the noiseless case. In such case the process quickly approaches an ergodic behavior and the considerations made in Section 4 for the noiseless case still hold.

As far as the uniformity degree of the obtained ergodic pdf ϕ^* is concerned, in all the tested cases the presence of noise caused the error to be attenuated with respect to the noiseless case in almost the entire domain $(0, 1]$ (Fig. 8 and 9). In detail this result indicates that for given parameter values B and α, the white internal noise substantially makes the stationary pdf *better uniformly shaped than in the noiseless case*, even if, from a qualitative point of view, the overall trend of the uniformity error function remains unchanged.

6.2 The invariant density of the final process

Once the samples $\{z'_m = z_m + BP\}$ are collected at the output of the analog block implementing the chaotic map, the signal is processed by linear blocks, and the overall effect of the additive external noise can be condensed into the sequence of random variables $\{\nu_m\}$ depicted in Fig. 1. In this subsection we assume the ergodic process $\{x_m = G(z'_m + \Delta)\}$ distributed according to the invariant pdf ϕ^*_x.

Assuming the external noise as an ergodic process of i.i.d. random variables, recalling eq. (8) we have that the stationary pdf ρ for the random samples $\{s_m\}$ (i.e., the samples used for the CDT) is given by the convolution of the ergodic pdf ϕ^*_x with the stationary pdf f_ν of the noise process. If again we assume the noisy samples $\{\nu_m\}$ to be Gaussian distributed with zero mean and standard deviation σ_e, the effect of the external noise can be studied using the standard Fourier analysis. Indeed, considering the pdfs as 1D-signals, we have that the

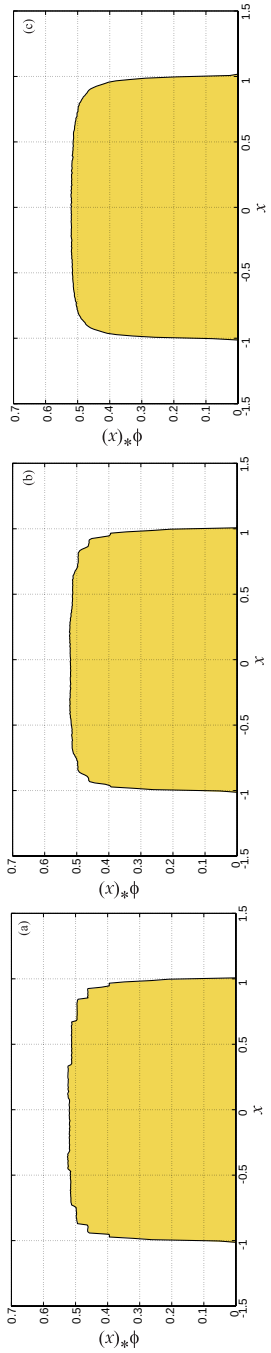


Figure 8: The effect of the internal noise on the shape of the ergodic pdf for the Sawtooth map with $B = 1.98$ and $\alpha = 0.001$: (a) noiseless case; (b) $\sigma_i = 0.25\sigma_{\max}$; (c) $\sigma_i = 0.75\sigma_{\max}$.

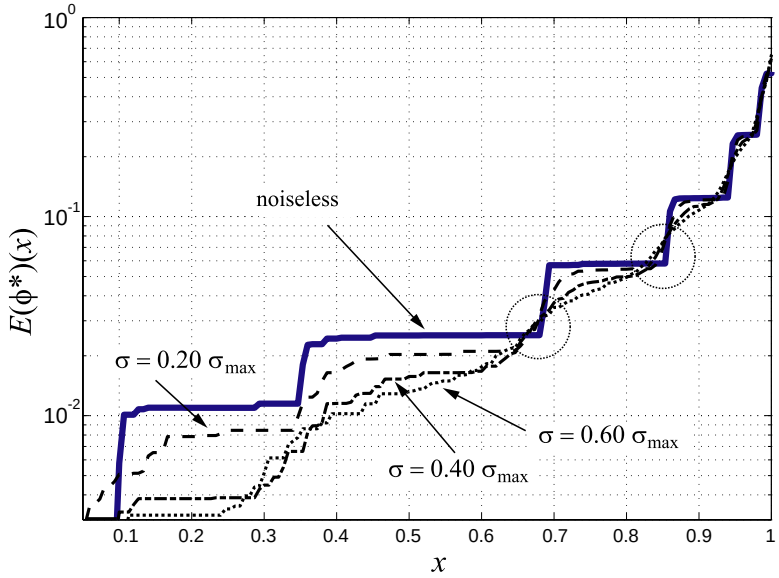


Figure 9: Thanks to the internal noise the uniformity error result to be attenuated with respect to the noiseless case in almost the entire domain $(0, 1]$ (the curves were estimated for the Sawtooth map with $B = 1.98$ and $\alpha = 0.001$). The circles highlight two limited regions in which the error is slightly worsened with respect to the noiseless case.

spectrum of ρ is given by the product of the spectrum of ϕ_x^* and the spectrum of f_ν. Since the Fourier transform of a Gaussian-shaped signal is again Gaussian shaped[9], the effect of the convolution is a Gaussian-shaped low-pass filtering of the original pdf ϕ_x^*, with a cutting frequency that is inversely proportional to the standard deviation of the noise process.

As a result, the low-pass filtering smooths the input pdf ϕ_x^*, similarly to what happens due to the internal noise previously discussed. Substantially, as confirmed by numerical simulations, the resulting qualitative effect of the external noise is equal to the one of the internal noise, with the difference that the former does not affect directly the chaotic dynamics. As it is discussed in what follows, if the internal noise and the external noise have comparable powers, the external noise does not significantly affect the shape of the pdf (i.e., in practice the resulting error function mainly depends on the internal noise). For $B > 1.9$ and $\sigma_i < 0.6\sigma_{\max}$ a linearized simplified reliable model for taking into account this behavior is reported in Fig. 10, where

$$H(f) \approx e^{-2\pi^2(\sigma_e^2+100\sigma_i^2)f^2}. \tag{43}$$

The previous expression is heuristic, it is based on simulation results, and it can be used for analyzing the global effect of noise. It is interesting noting that the effect of the internal noise is approximately 10 times more important than the one produced by the external noise. Summarizing, if $\sigma_e \approx \sigma_i$ (as it is expected

[9] We recall that $\frac{1}{\sigma_e\sqrt{2\pi}} e^{-\frac{x^2}{2\sigma_e^2}} \overset{\mathcal{F}}{\longleftrightarrow} e^{-2\pi^2\sigma_e^2 f^2}$.

in analog circuits), the shape of the final pdf is *substantially determined by the internal noise only.*

7 Analysis of E2 errors for the CDT and performance evaluation

As discussed in Section 3, the uncertain knowledge of the ergodic pdf ρ associated with the input samples $\{s_m\}$ used in the CDT cause inaccurate estimations of the transition levels. In this section we want to relate the uniformity error (30) of ρ with the accuracy of the CDT once *assuming the ergodic process* $\{s_m\}$ *uniformly distributed* between the transition levels $V_T(1)$ and $V_T(N)$ of the ADC under test.

Accordingly, we suppose that over the interval $(V_T(1), V_T(N))$ the pdf ρ is affected by an uniformity error ε, i.e., we assume that

$$(V_T(1), V_T(N)) = (-U(\varepsilon), U(\varepsilon)) \tag{44}$$

and therefore $\overline{Q} = \frac{2U(\varepsilon)}{2^n-2}$. In other words, the input range of the ADC determines the subinterval (44) of the chaotic domain in which the inequality (34) in true.

Similarly to what discussed in Section 3 for uniformly distributed samples, the estimation $\tilde{V}_T(k)$ of the k-th transition level for $k = 1, \ldots, N$ can be written as

$$\tilde{V}_T(k) = -U_\varepsilon + \lim_{S_\# \to \infty} \frac{2U_\varepsilon}{S_\#} \sum_{i=1}^{k-1} \frac{h_S(i)}{\Pi}, \tag{45}$$

where

$$\Pi = \int_{-U_\varepsilon}^{U_\varepsilon} \rho(x)dx = 2U_\varepsilon \overline{\rho}(U_\varepsilon). \tag{46}$$

The above quantity Π represents the ratio of samples that fall between the first and the last transition level, and therefore we call it the *efficiency of the ergodic process.* It is worth noting that the quantity

$$\lim_{S_\# \to \infty} \frac{h_S(k)}{S_\# \cdot \Pi} \tag{47}$$

is equal to the conditioned probability

$$\begin{aligned} P\left\{x \in (V_T(k),\ V_T(k+1)) \,|x \in (-U_\varepsilon, U_\varepsilon)\right\} = \\ = \frac{\int_{V_T(k)}^{V_T(k+1)} \rho(x)dx}{\int_{-U_\varepsilon}^{U_\varepsilon} \rho(x)dx} = \frac{\mu(I_k)}{\Pi}, \end{aligned} \tag{48}$$

where I_k denotes the interval $(V_T(k), V_T(k+1))$, that is the support of the k-th code bin. Therefore, eq. (45) can be rewritten as

$$\tilde{V}_T(k) = -U_\varepsilon + \frac{2U_\varepsilon}{\Pi} \sum_{i=1}^{k-1} \mu(I_i), \tag{49}$$

and according to (1) we have

$$\tilde{W}(k) = \tilde{V}_T(k+1) - \tilde{V}_T(k) = \frac{2U_\varepsilon}{\Pi} \mu(I_k) = \frac{\mu(I_k)}{\overline{\rho}(U_\varepsilon)}. \tag{50}$$

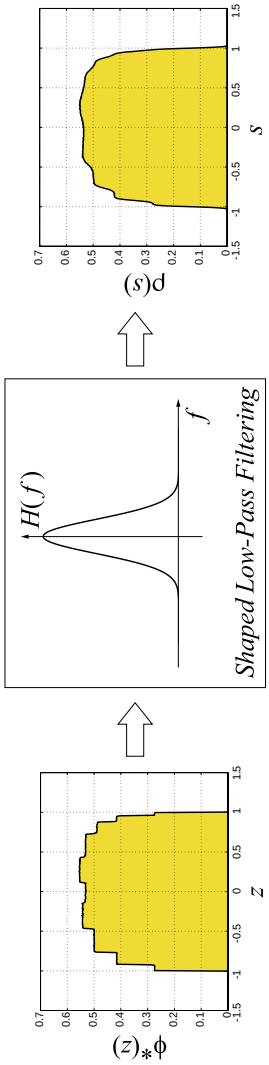


Figure 10: Simplified linear model for taking into account the global effect of noise (internal and external).

7.1 Accuracy in the estimation of the DNL and INL errors

We start assuming to test an ideal n-bit ADC, i.e., we suppose $V_T(k+1) = V_T(k) + \overline{Q}$, for $k = 1, \ldots, 2^n - 1$, with $\overline{Q} = \frac{V_T(2^n-1) - V_T(1)}{2^n - 2}$. Consequently, the ADC under test has $\mathrm{DNL}_{\max} = \mathrm{INL}_{\max} = 0$. In such case, we note that it results

$$\lambda(I_k) = V_T(k+1) - V_T(k) = \overline{Q}. \tag{51}$$

We are interested in quantifying the accuracy for the estimation of the DNL and INL errors, and to this aim we adopt the approximated expressions discussed in the Section 2, i.e., we are assuming for the device under test $\Gamma \approx 1$ and $V_{OS} \approx 0$.[10]

Accordingly, for the ideal ADC under test we can estimate

$$\begin{aligned} \tilde{\mathrm{DNL}}(k) &\approx \frac{\tilde{W}(k) - \overline{Q}}{\overline{Q}} = \\ &= \frac{\frac{\mu(I_k)}{\overline{\rho}(U_\varepsilon)} - \lambda(I_k)}{\lambda(I_k)} = \frac{\mu(I_k) - \overline{\rho}(U_\varepsilon)\lambda(I_k)}{\overline{\rho}(U_\varepsilon)\lambda(I_k)}. \end{aligned} \tag{52}$$

Since $I_k \subset (-U(\varepsilon), U(\varepsilon))$ we can use Theorem 2, finally obtaining

$$|\tilde{\mathrm{DNL}}(k)| \leq \varepsilon. \tag{53}$$

Since this holds for all k then

$$\tilde{\mathrm{DNL}}_{\max} \leq \varepsilon. \tag{54}$$

Concluding, using eq. (6) it results $\tilde{\mathrm{INL}}(k) \approx -\sum_{i=0}^{k-1} \tilde{\mathrm{DNL}}(i)$ that implies

$$\tilde{\mathrm{INL}}_{\max} \leq 2^n \varepsilon. \tag{55}$$

Assuming to test an ideal n-bit ADC, the relationships (54) and (55) represent two asymptotic[11] worst case upper bounds for the inaccuracy in the estimation of the DNL and INL errors when using in the CDT an ergodic process with a uniformity distribution error level ε. Moreover, it is worth noting that (55) is widely overestimated since the result was obtained assuming $\tilde{\mathrm{DNL}}(k) = \varepsilon$ for all k.

7.2 The general case

The inequality (54) was determined under the hypothesis of testing an ideal ADC. As far as the DNL error is taken into account, starting from (5), in the general case we can write

$$\mathrm{DNL}(k) = \frac{W(k) - \frac{\overline{Q}}{\Gamma}}{\frac{\overline{Q}}{\Gamma}} = \frac{W(k) - \overline{Q}'}{\overline{Q}'}, \tag{56}$$

[10] The assumption holds since we are assuming the device under test as an ideal one, and supposing reasonable small uniformity errors of the ergodic pdf. The validity of the reasoning is then discussed and supported with examples in the next Section.

[11] The term 'asymptotic' derives from the assumption of using for the CDT an infinite sequence of input samples.

and therefore, using (50) and Theorem 2 we have

$$\left|\tilde{\mathrm{DNL}}(k) - \mathrm{DNL}(k)\right| = \left|\frac{\frac{\mu(I_k)}{\overline{\rho}(U_\varepsilon)} - \overline{Q}'}{\overline{Q}'} - \frac{\lambda(I_k) - \overline{Q}'}{\overline{Q}'}\right| =$$

$$= \frac{1}{\overline{Q}'}\left|\frac{\mu(I_k) - \lambda(I_k)\overline{\rho}(U_\varepsilon)}{\overline{\rho}(U_\varepsilon)}\right| \leq \frac{\varepsilon\lambda(I_k)}{\overline{Q}'} = \frac{\varepsilon\Gamma\lambda(I_k)}{\overline{Q}}. \tag{57}$$

It is worth noting that if the ADC under test is ideal, inequality (53) and (57) become exactly the same[12]. The above result assure the reliability of the method in the general case, showing that an upper bound for the error in the estimation of the DNL exists. Since the upper bound directly depends on ε, changing the efficiency Π of the ergodic process the accuracy of the method can be arbitrarily enhanced, as discussed in the following subsection.

7.3 The trade off between accuracy and efficiency

Referring to the properties of the uniformity error function (30) discussed in subsection 5.1, it is interesting noting that since $\lim_{x\to 0^+} E(\rho)(x) = 0$ the uniformity error level ε can be set arbitrarily small, obtaining for the CDT any desired asymptotic accuracy in the estimation of the DNL and INL errors. Nevertheless, as clearly indicated by the plots in the second row of Fig. 6, due to the growing trend of $E(\rho)$, the smaller is ε and the smaller is U_ε defined in (33), i.e., the smaller is the subinterval of the chaotic domain that is used for the test, with a resulting decrease of the efficiency Π of the ergodic process defined in (46). In other words, if the stationary pdf of the ergodic source is not perfectly uniformly shaped, the ratio of samples that fall between the first and the last transition level drops to zero as far as $\varepsilon \to 0$. This fact in practice causes an increase of the time required to perform the CDT by a factor of $1/\Pi$, i.e., if for examples 10^6 samples are required for the CDT, then $10^6/\Pi$ samples have to be generated (in average).

The above issue can be explained in more familiar terms introducing the following

Definition 3 *Let the ergodic pdf ρ be distributed over $[-L, L)$ and let the first and last nominal transition levels of the ADC under test be $-u$ and u respectively*[13]*, with $u \leq L$. The quantity $\Omega = L/u$ is called the* overdrive *of the input ergodic source.*

In the next Section a further discussion on this point is provided.

Let now assume that the ergodic source is based on a non-diverging chaotic Sawtooth map. On the basis of what previously discussed, we have the following property: *for any $\varepsilon > 0$ an overdrive Ω exists such that the obtained E2 error levels in the CDT are smaller than ε.*

We conclude this section noting that if the input pdf ρ is reasonably close to the uniform pdf (e.g., the Sawtooth map with $B > 1.94$ and with a moderate presence of noise), then $\rho(x) \approx \frac{1}{2L}$ and the efficiency of the ergodic process is related to the overdrive by the approximated relationship $\Pi \approx \frac{1}{\Omega}$.

[12] Indeed, the ideal ADC has $\mathrm{DNL}(k) = 0$ for all k, $\Gamma = 1$, $\lambda(I_k) = \overline{Q}$.

[13] The setup has general validity, since the ergodic process can be scaled and centered anywhere in the real domain.

8 Examples and Final Remarks

In this section we discuss two experiments based on real chaotic sequences generated by a Sawtooth circuit prototype, following the approach presented in [5]. The prototype was implemented using a field programmable analog array (FPAA, Anadigm AN212E04), that is a SRAM-based device that allows for designing low/medium complexity switched-capacitor circuits by exploiting a library of fully differential blocks.

We stress that in order to assess the reliability of the proposed CDT method, an *a priori* perfectly known ADC would be required for being tested. Since no real device could be used for this purpose, we referred to two *virtual* 10 bit ADCs, i.e., we referred to two simulated artificial devices in which the nonidealities could be set at will. In order to test the two virtual ADCs we acquired the chaotic sequences using a National Instruments USB-6251 16 bit ADC[14].

For both of the experiments we adopted the following scheme:

1. we defined the static transfer function of the virtual ADC under test. In order to simulate a real device, a proper algorithm was developed for introducing in the transfer function random errors (e.g., gain and nonlinearity errors);

2. on the basis of the actual transfer function of the virtual ADC, the actual gain error, the actual offset error, the actual INL error and the actual DNL errors were computed referring to the definitions introduced in Section 2;

3. to perform the CDT we used real 10^6 samples[15] generated by a Sawtooth circuit prototype and acquired using a 16 bit ADC. Depending on the required DNL estimation accuracy, by properly setting the parameter G in Fig. 2, the overdrive for the input ergodic source was set in agreement with the uniformity error function (30) of the stationary distribution.

4. by means of the CDT we obtained the estimations for the gain error, the offset error, the INL error and the DNL errors. The estimations were then compared with the actual quantities previously computed.

For the virtual ADCs under test, the nominal full scale of the converters was supposed to range between $-1V$ and $+1V$. For the implemented ergodic source it was found that $B \geq 1.95, \alpha \leq 2 \cdot 10^{-3}$ $\sigma_i \approx \sigma_e = 0.5\sigma_{\max} \approx 20mV$ (see the Appendix and [5, 12, 13]).

In Fig. 11 the simulated stationary distribution of an ergodic source with $B = 1.95, \alpha = 2 \cdot 10^{-3}$, $\sigma_i \approx \sigma_e = 0.5\sigma_{\max} \approx 20mV$ is reported. In the same figure, the respective uniformity error function is plotted (overdrive not applied).

According to the uniformity error function of Fig. 11, by setting for the DNL estimation accuracy $\varepsilon = 0.02$, an U_ε level approximately equal to 0.38 is obtained. Accordingly, to cover the virtual ADC full scale range, the interval $(-U_\varepsilon, U_\varepsilon)$ was expanded by setting an overdrive $\Omega \approx 2.6$, obtaining an ergodic source efficiency $\Pi \approx 40\%$.

[14] The resolution of the two virtual ADCs under test (10 bit) was chosen in order to make sure that the experiment results were not depending on the errors introduced by the real 16-bit ADC used to acquire the chaotic sequences.

[15] It is worth noting that the number of samples was chosen large in order to make the results almost not dependent on the type E1 errors.

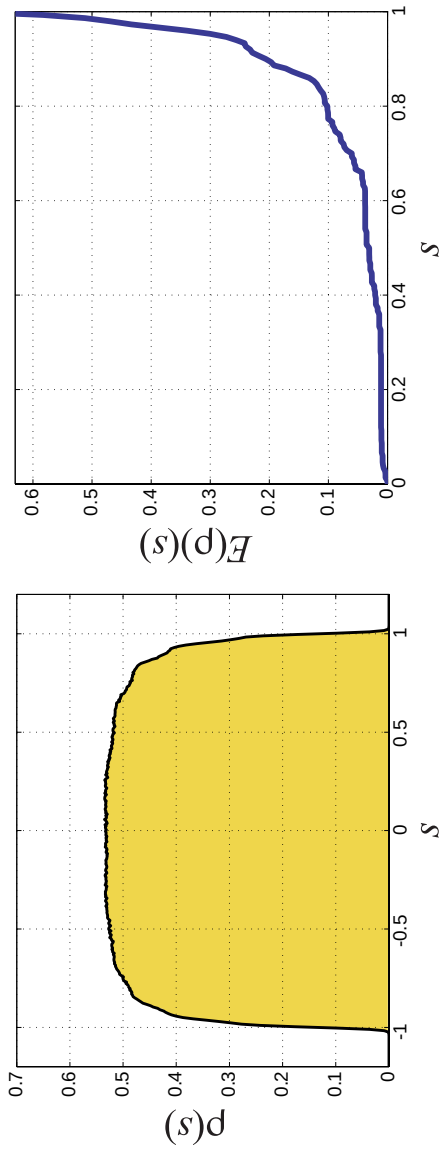


Figure 11: The stationary distribution of an ergodic source with $B = 1.95, \alpha = 2 \cdot 10^{-3}$, $\sigma_i \approx \sigma_e = 0.5\sigma_{\max} \approx 20mV$, and its uniformity error function (before applying overdrive).

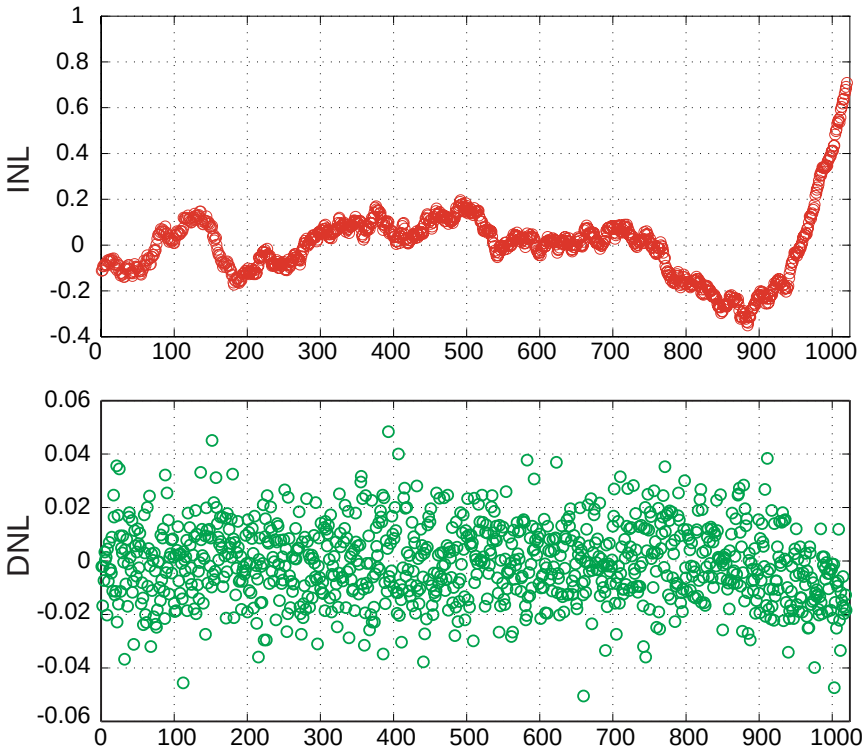


Figure 12: INL and DNL estimation for a 10-bit ideal ADC using for the CDT a sequence of 10^6 samples generated by the chaotic Sawtooth map.

8.1 Example 1: test of an ideal 10-bit ADC

In this example the CDT of an ideal 10-bit ADC was simulated. In such case $\Gamma = 1, V_{OS} = 0$ and $\mathrm{DNL}_{\max} = \mathrm{INL}_{\max} = 0$. The outcomes of the experiment yielded for the gain and offset estimation $\tilde{\Gamma} \approx 0.9963$ and $\tilde{V}_{OS} \approx -0.0035V$, whereas the INL and DNL error estimations are reported in Fig. 12. The results confirm the theoretical analysis about the estimation accuracy discussed in the previous Section, and the obtained small INL estimation error (< 0.8 for the higher output codes) gives an idea about the strong overestimation of the worst case upper bound (57).

8.2 Example 2: test of a non-ideal 10-bit ADC

In this example a non-ideal 10-bit ADC was considered with $\Gamma = 0.9439, V_{OS} = -0.0518$ and INL and DNL errors reported in the left column of Fig. 13 (due to the gain error, the actual number of output codes is lower than 1024). The outcomes of the experiment yielded for the gain and offset estimation $\tilde{\Gamma} \approx 0.9420$ and $\tilde{V}_{OS} \approx -0.053V$, whereas the INL and DNL error estimations are reported in the right column of fig. 13. Also in this case the results confirm the theoretical analysis about the estimation accuracy discussed in the previous Section. The INL estimation error (< 0.8 for the higher output codes) is in accordance with

the ideal case previously discussed, and indicates a systematic error that is related to the non-uniform shape of the stationary density of the ergodic source used in the experiment.

8.3 Final remarks

The two previous examples confirm the reliability of the method, that gives acceptable results even using for the ergodic source parameter values typically obtained when the chaotic system is implemented by non optimized hardware prototypes [5, 12, 13]. Due to the high sensitivity of the shape of the stationary distribution to small parameter changes, whatever improvement in the implementation accuracy (that allows, e.g., parameter B to reach levels equal to 1.96 or 1.97) assures a significant decrease of the uniformity error (see Fig. 6), with a consequent increase of the ergodic source efficiency or, conversely, a consequent increase of the accuracy in the estimation of the ADC transition levels.

9 Conclusions

In this paper the use of the chaotic Sawtooth map for the generation of signals with predefined statistical characteristics is proposed for testing ADCs. Referring to the CDT, the main idea is to exploit the ergodic stochastic process ruled by the Sawtooth dynamical system as a source of almost-uniform distributed samples. The proposed solution is analyzed and discussed from a theoretical point of view, and a method for evaluating the uniformity degree of the obtained distribution of samples is introduced. The method is based on the definition of the uniformity error function (30) that has a general validity and does not depend on the specific chaotic system proposed in this paper. Among the chaotic dynamical systems, the Sawtooth map exhibits a statistical behavior that can be easily corrected and controlled according to the feedback strategy discussed in [5] and briefly reviewed in the Appendix. Theoretical results, also supported by the two experiments discussed in Section 8, confirm the reliability of the proposed solution, showing that chaotic systems can represent an alternative for the generation of signals to be used in the CDT of ADCs.

References

[1] "IEEE Std 1241-2000 – IEEE Standard for Terminology and Test Methods for Analog-to-Digital Converters," available online at http://www.ieee.org/, 2001.

[2] P. G. A. Jespers, *Integrated Converters*. Oxford University Press, 2001.

[3] J. Blair, "Histogram measurement of adc nonlinearities using sine waves," *IEEE Trans. Instrum. and Meas.*, vol. 43, no. 3, pp. 373–383, 1994.

[4] T. Addabbo, A. Fort, S. Rocchi, D. Papini, and V. Vignoli, "Invariant measures of tunable chaotic sources: Robustness analysis and efficient estimation," *IEEE Transactions on Circuits and Systems - I*, vol. 56, no. 4, pp. 806–819, Apr. 2009.

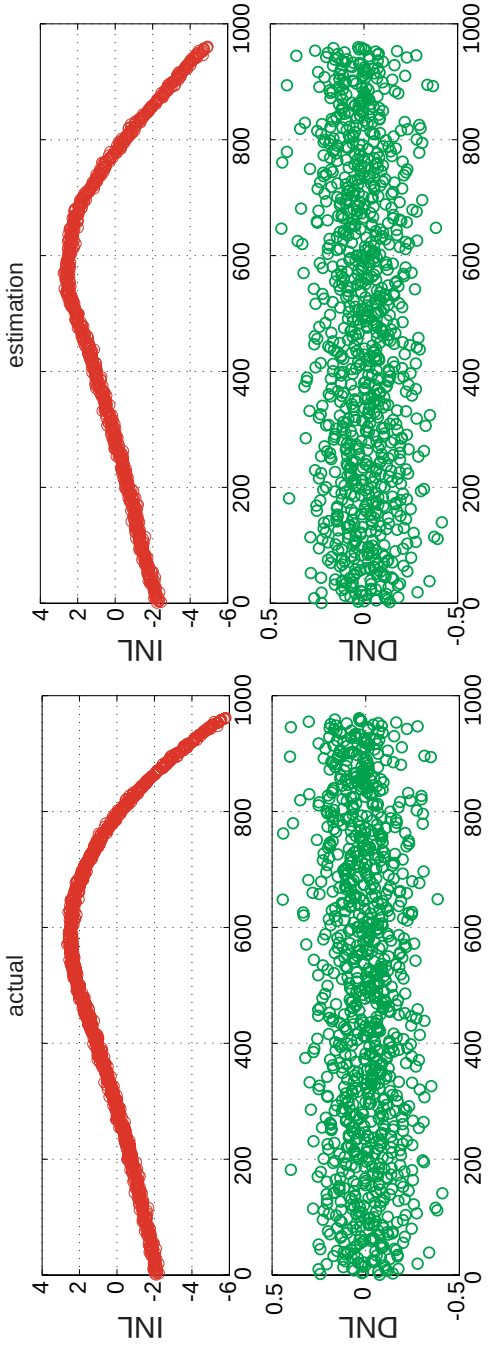


Figure 13: Actual INL and DNL errors (left) and their respective estimation (right) for a 10-bit non ideal ADC using for the CDT a sequence of 10^6 samples generated by the chaotic Sawtooth map.

[5] T. Addabbo, M. Alioto, A. Fort, S. Rocchi, and V. Vignoli, "A feedback strategy to improve the entropy of a chaos-based random bit generator," *IEEE Transaction on Circuits and Systems – part I*, vol. 53, no. 2, pp. 326–337, 2006.

[6] A. Lasota and M. C. Mackey, *Chaos, Fractals and Noise - Stochastic Aspects of Dynamics*, 2nd ed. Springer, 1994.

[7] T. Stojanovski and L. Kocarev, "Chaos-based random number generator – part I: Analysis," *IEEE Transactions on Circuits and Systems I*, vol. 48, no. 3, pp. 281–288, 2001.

[8] A. Boyarsky and P. Góra, *Laws of Chaos.* Birkhäuser, 1997.

[9] R. Devaney, *An Introduction to Chaotic Dynamical System*, 2nd ed. Addison-Wesley, 1989.

[10] T. Addabbo, A. Fort, D. Papini, S. Rocchi, and V. Vignoli, "An efficient and accurate method for estimation of entropy and other dynamical invariants for piecewise affine choatic maps," *International Journal of Bifurcation and Chaos*, 2009, (Accepted).

[11] F. Pareschi, G. Setti, and R. Rovatti, "Noise robustness condition for chaotic maps with piecewise constant invariant density," in *ISCAS 2004*, vol. IV, 2004, pp. 681–684.

[12] T. Addabbo, M. Alioto, A. Fort, S. Rocchi, and V. Vignoli, "Entropy enhancement in a chaos-based random bit generator," in *NOLTA 2006, Proceedings of the 2006 International Symposium on Nonlinear Theory and its Applications*, BOLOGNA (ITALY), Sep. 2006, pp. 375–378.

[13] ——, "Uniform-distributed noise generator based on a chaotic circuit," in *IMTC 2006, Proceedings of the 23rd IEEE Instrumentation and Measurement Technology Conference*, SORRENTO (ITALY), Apr. 2006, pp. 1156–1160.

Appendix – A method for controlling the Sawtooth map parameters

The method proposed in [5] for controlling the parameters of the Sawtooth map, adapted for the CDT purposes, is briefly reviewed in this appendix. Referring to the block diagram of Fig. 2, in [5] it was proved that the parameters B and α of the Sawtooth map can be controlled using two N_c-bit digital signals C_B and C_α (the authors showed in [5] that in practical cases $N_c = 5$ suffices for obtaining a reliable quality of the control). The digital codes for C_B and C_α are determined analyzing the digital output of the comparator $\{Y_m\}$, where $Y_m = 1$ if $z_m \geq P$ and $Y_m = 0$ otherwise.

Using a successive approximation strategy, the aim of the algorithm described by the simplified flowchart in Fig. 14 is both to set $|\alpha|$ below a small worst case value $|\alpha|_{wc}$ and, according to (17), to bring the parameter B as much as possible close to 2, above the worst case value $B_{wc} = \frac{2}{1+|\alpha|_{wc}} < 2$ [12]. This

result must be accomplished avoiding the system diverging, i.e., avoiding that at the end of the correction procedure $\sigma_i \geq 0.6\sigma_{\max}$. In principle, in the noiseless case the higher is the accuracy of the digital signals C_B and C_α, and the more B gets close to 2. In practical circuits the worst case bound is a function of the noise level that sets an upper limit to the accuracy of the correction system (Fig.15).

The controlling algorithm alternates two phases, the first for reducing $|\alpha|$, and the second for increasing B. The decisional core of the algorithm is based on the 'count the ONES' statistical operation, which is used for evaluating the unbalancing of the chaotic sequence. Since this latter operation depends on the statistics of the output, the result of the correction is probabilistic. The divergence detection can be achieved in several ways, since in electronic circuits a divergence orbit is typically attracted toward a parasitic fixed point introduced by the saturation of amplifiers [7], (i.e., the comparator in the block diagram of Fig. 2 issues in this case a fixed symbolic sequence [5]). In [5] the authors used this correction procedure achieving satisfactory results by setting $L = 8192$ bits in the count the ONES statistical operation, and with $N_C = 5$. Taking into account all the iterations of the algorithm, the method corrects the Sawtooth map parameters using less than 500.000 output samples.

Once the successive approximation strategy is completed the control system periodically performs a further fine re-tuning of the system parameters in order to counteract possible drifts of gains and offsets in the analog circuit (e.g., due to temperature fluctuations), or in order to restore the system behavior after occasional divergence events caused by noisy peaks. Summarizing, the overall correction and control system requires a counter, a few more logic blocks and two digital to analog converters to be interfaced with the analog circuit implementing the chaotic map (i.e., the first for setting the reference level of the comparator, and the second for setting the variable gain of the amplifier block B). The correction algorithm has been tested to control a Field Programmable Analog Array (FPAA Anadigm AN212E04), obtaining typical B values greater than or equal to 1.95 when referring to standard student-level experimental setup, in which no particular precaution was taken to limit the presence of noise [5,12,13].

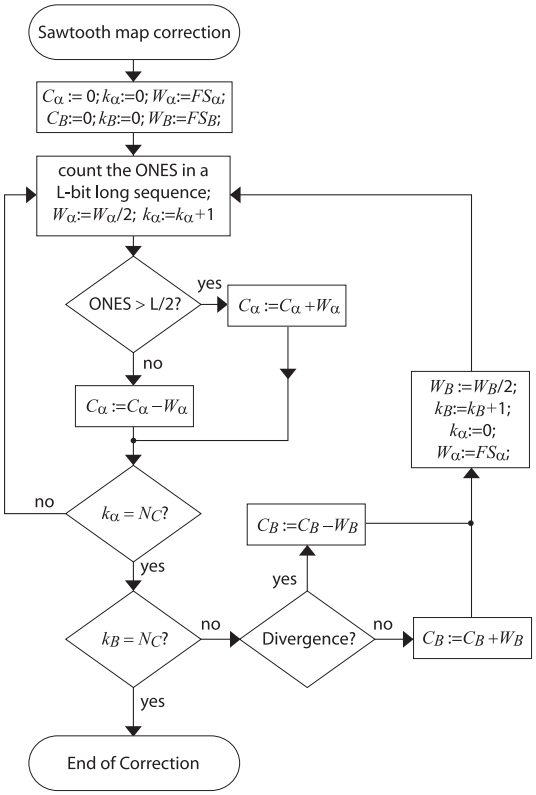


Figure 14: Simplified flowchart of the Sawtooth map correction algorithm. The constants FS_α and FS_β represents the full scale of the correction signals for α and β respectively. N_C is the digital resolution (number of bits) used for the correction signals C_α and C_β.

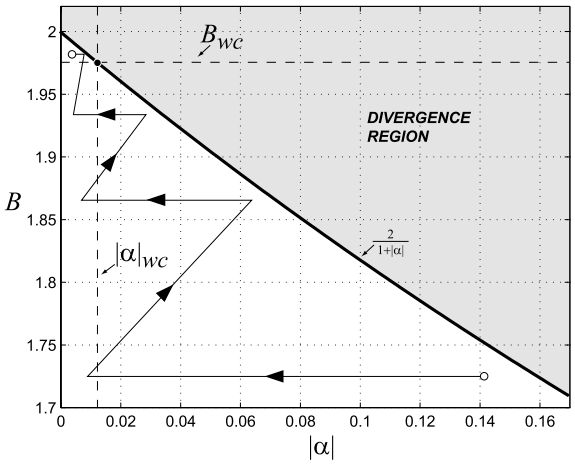


Figure 15: Schematic running of the procedure for correcting the parameters B and α.